



Universiteit
Leiden
The Netherlands

Beyond perfusion: measuring water transport across brain barriers with arterial spin labeling MRI

Petitclerc, L.

Citation

Petitclerc, L. (2023, November 14). *Beyond perfusion: measuring water transport across brain barriers with arterial spin labeling MRI*. Retrieved from <https://hdl.handle.net/1887/3657163>

Version: Publisher's Version

License: [Licence agreement concerning inclusion of doctoral thesis in the Institutional Repository of the University of Leiden](#)

Downloaded from: <https://hdl.handle.net/1887/3657163>

Note: To cite this publication please use the final published version (if applicable).

Chapter 1

General Introduction

1.1 THE BLOOD-BRAIN BARRIER

1.1.1 Definition and Relevance

The blood-brain barrier (BBB) is a boundary between the blood flowing in the vasculature and the brain tissue which it perfuses. It serves a number of functions, namely the preservation of the tissue microenvironment homeostasis (i.e. the equilibrium of ions and molecules which are involved in brain function), the transport of nutrients from blood to tissue, and the protection of neuronal tissue from any pathogens or other harmful products which could be present in the blood.¹⁻⁴ This boundary resides at the level of the endothelium which lines the blood vessels and capillaries of the brain. In most organs of the body, there are physical gaps present between such endothelial cells which allow bulk flow of water and its solutes between blood and tissue. However, in the brain, endothelial cells are bound together with tight junctions restricting bulk flow of water, which instead exchanges across the BBB through a process of facilitated diffusion. Molecules and ions which are necessary for brain function cross the BBB through designated transporters present in endothelial cell walls.

Proper BBB function is of great importance to ensure the continuous influx of nutrients to brain tissue, and to protect the central nervous system (CNS) from disease. Disruption of the BBB structural integrity can lead to infection by letting through bacteria and viruses, but it is also associated with a large number of other neurological disorders. Breakdown of the BBB in the form of increased permeability has been observed in acute conditions such as stroke⁵ and tumours⁶ as well as chronic neurodegenerative disorders such as Alzheimer's Disease⁷⁻⁹, dementia¹⁰, Parkinson's Disease and Multiple Sclerosis², among others. Additionally, the BBB and the transporters which allow movement of water and molecules across it are altered in the normal aging process of the brain¹¹. Thus, there appears to be a close and complex relationship between disease and BBB disruption, and in some cases, it is not yet clear whether BBB breakdown appears as a cause of disease or as a consequence. Accurate characterization of BBB function is important as it allows us to elucidate this relationship, monitor the progression of disease, and make informed treatment decisions for patients with disorders of the CNS.

1.1.2 Characterizing the Blood-Brain Barrier

Traditionally, the techniques of choice to characterize BBB permeability are dynamic contrast-enhanced (DCE) MRI, contrast-enhanced computed tomography (CE-CT) or positron emission tomography (PET).^{10,12,13} In these techniques, a contrast agent is injected intravenously and the related signal in blood and tissue before and after injection are measured. In the case of DCE-MRI, which is the most common of these techniques, a number of contrast agents can be used. These are all molecules that contain gadolinium (Gd), an element which is paramagnetic, modifying the T_1 and T_2 water relaxation times in local tissue.

It is this change in T_1 and T_2 that is measured and provides contrast in DCE-MRI. The word “dynamic” in DCE-MRI is particularly important because what is imaged is the dynamic inflow of contrast agent into the cerebral vasculature, followed by transport across the BBB and/or efflux from the brain. Therefore, measurements at multiple time points are needed. This can simply take the form of pre- and post-injection images, or alternatively sequential acquisition of multiple frames starting immediately before injection. By measuring the signal intensity in blood and tissue before injection and over time afterwards, an MR physics-based model is used to extract the concentration of contrast agent at every time point. These concentration-time curves in blood and tissue are fitted to a compartmental model to extract the volume transfer constant from blood to brain, K_{trans} (alternative terms are K_1 or the permeability-surface (PS) product) in units of min^{-1} , with a larger K_{trans} indicating a more permeable BBB.^{14,15}

Although DCE-MRI is currently the most-used standard for BBB assessment, Gd-based permeability measurements have some limitations. Firstly, while they are small in the grand scheme of molecular biology, the contrast agent scaffolds are comparatively large compared to water or other molecules which are transported across the BBB in the healthy brain. Consequently, Gd-based contrast agents do not cross the healthy BBB.¹⁶ This means that measuring BBB leakage with these contrast agents may overlook more subtle changes in permeability to smaller molecules when damage to the barrier is non-existent or limited. Secondly, there are mounting concerns with the possibility of gadolinium deposition in (brain) tissue over time from repeated injections of Gd contrast agents, as well as the risk for development of nephrogenic systemic fibrosis if the contrast agent dechelates.¹⁷⁻²⁰ However, especially cyclic Gd-based contrast agent are still considered relatively safe, when considering their value in diagnosing brain diseases.

Increasingly, water is seen as an alternative contrast for BBB measurements, which presents a lot of advantages. Water exchanges across the BBB as part of a number of natural transport mechanisms, and it is an innate source of MRI contrast that does not require invasive injections. It is therefore also more feasible to perform repeated or longitudinal measurements, and its small size should theoretically allow for measurements of more subtle BBB damage.¹⁴ Changes in BBB permeability to water could therefore be an earlier biomarker for BBB breakdown than measurements based on Gd contrast agents. Arterial spin labelling (ASL) is the technique of choice to measure water exchange across the BBB, because it specifically labels the blood water and allows its tracking from the vessels to the tissue. Section 1.4 of this thesis gives an introduction to ASL and **chapter 2** delves into more detail about BBB characterization techniques using ASL.

1.2 CEREBROSPINAL FLUID AND BRAIN CLEARANCE

1.2.1 The Problem of Waste Clearance in the Brain and the Role of CSF

Every organ in the human body produces waste in some form, and this waste is transported through the lymphatic system towards the appropriate treatment and excretion sites. The brain, although it has a high metabolic rate (discussed further in section 1.3) and therefore creates large amounts of waste products, does not however possess a traditional lymphatic system to perform this task. In fact, surprisingly little is known of the brain's waste clearance system, and it is the topic of much current research and at times heated debate in the neuroimaging community.^{21–25}

What is known about brain clearance is that it takes place through the cerebrospinal fluid (CSF) and interstitial fluid (ISF) instead of lymph. Once thought of mainly as a mechanical support for the brain (to protect from impact and afford buoyancy), CSF is now understood to have physiological relevance especially in the clearance of waste from the brain as well as in immune responses and delivery of nutrients. However, much remains to be understood about the exact processes by which CSF is produced, how it exchanges with ISF, and in general the pathways of movement of CSF through the brain.

The traditional hypothesis of CSF flow has been dubbed the “third circulation” by Harvey Cushing in 1925²⁶, as an analogue to the movements of blood and lymph, which travel unidirectionally through their vasculature in a closed circuit pattern. The idea is that the CSF, just like blood and lymph, circulates through the CNS unidirectionally from a source to a point of outflow. Under this hypothesis, the CSF is produced exclusively at the choroid plexus (CP), a small structure in the ventricles, by water and ions traversing the blood-CSF barrier (BCSFB). After the CSF is secreted, the third circulation dictates that it flows unidirectionally from the ventricles, down through the aqueducts into the spine and subarachnoid space (SAS) which surrounds the brain, before being reabsorbed into the blood by the arachnoid villi or granulations (structures along the dural venous sinuses).^{26,27} Figure 1.1 shows a schematic representation of the flow of CSF according to the third circulation.

There is, however, mounting evidence that this view is incomplete and CSF production and flow is much more complex.^{29–31} In fact, all three main components of the third circulation theory (CSF production by the CP, unidirectional flow, and outflow through the arachnoid villi) have been challenged by ongoing research. Studies in a number of animals have shown that, after full resection of the CP, some CSF production remains, necessitating the existence of other sources of CSF outside the CP, which appear to contribute significantly

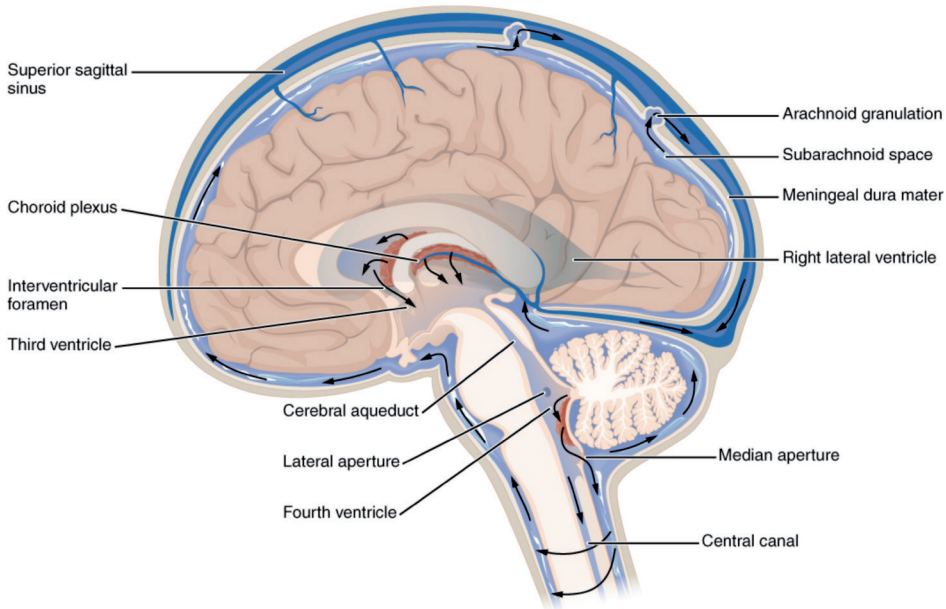


Figure 1.1. Flow patterns of CSF through the CNS according to the third circulation theory. (From Betts et al.28, this image is licensed under the Creative Commons Attribution 4.0 International license. <https://creativecommons.org/licenses/by/4.0/>)

to its production.^{32–34} Others have observed flow patterns of CSF that were more erratic and complex and did not correspond to unidirectional flow from the CP to the arachnoid villi, and have challenged the capacity of the CP to act as a pump which could sustain this flow.^{29,35–37} Finally, the reabsorption of the CSF into the arachnoid villi is also being brought into question as evidence of alternative routes for outflow has been found.³⁸ In this work, we will focus on the production of CSF through the BCSFB, which will be described in more detail in section 1.2.2.

1.2.2 The Blood-CSF Barrier and Water Exchange

The blood-CSF barrier is the boundary that regulates the exchange of water and other compounds between the blood and CSF. Primarily, it acts as the site of production of CSF and therefore plays an important role in brain waste clearance. It is usually understood to be concentrated at the choroid plexus, a small structure situated in all four of the human brain's CSF-filled ventricles. The CP is highly vascularized and lined with a specific type of epithelial cells with a folded surface that maximizes the area of contact between the CP and the CSF for more efficient exchange between blood and CSF. These cells are bound together by tight junctions to prevent bulk flow and transport of unwanted molecules, and their walls contain the transporters responsible for water transport and ion regulation in the CSF.^{39–41} The BBB and the BCSFB, although they share similar functions of protection of

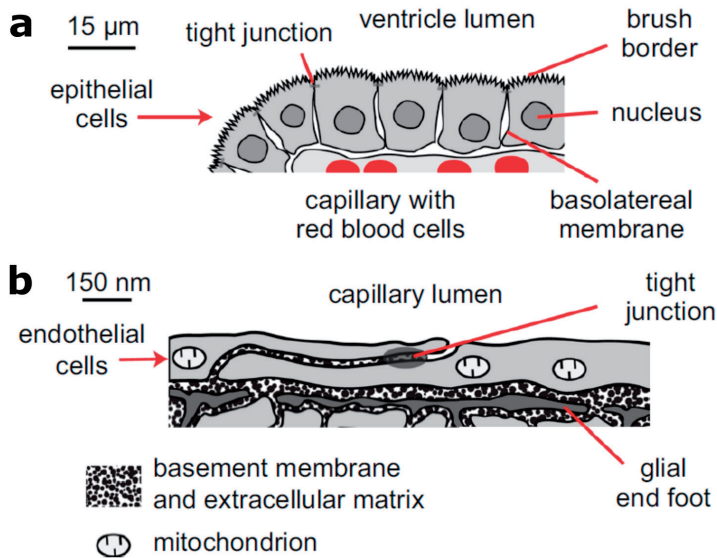


Figure 1.2. Comparison of the structures of the BCSFB (a) and the BBB (b). (Adapted from Hladky et al.⁴¹ This article is distributed under the terms of the Creative Commons Attribution 4.0 International License (<http://creativecommons.org/licenses/by/4.0/>))

the CNS and preservation of homeostasis, differ significantly in their structures, anatomical positions, and roles. Notably, the BBB's tight junctions between endothelial cells lining the microvasculature of almost the entirety of the CNS are absent from the CP, where fenestrated capillaries are instead present, with tight junctions between epithelial cells (see figure 1.2).

As discussed previously, there is evidence of extrachoroidal sources of CSF production in the brain. Emerging theories explain this by positing the secretion by the BBB of fluid, which joins the interstitial fluid (ISF) surrounding tissue cells and mixes with CSF at the level of perivascular spaces (PVS). PVS are CSF-filled spaces surrounding blood vessels in the brain.^{41,42} Although it is known that water and ions which form the CSF can exchange at the BBB, evidence of net production of fluid at the BBB is currently lacking.

Numerous methods have been proposed over time for the measurement of CSF production (by the CP or otherwise).³¹ In large part, traditional methods are very invasive, requiring surgical implants or lumbar puncture. As such, in many cases these are not performed in humans and mainly preclinical animal studies have been published. Alternatively, new MRI techniques allow non-invasive measurements of the flow of CSF through the aqueduct with phase-contrast imaging⁴³⁻⁴⁵ and the so-called time-SLIP method⁴⁶, which relate to the rate of CSF production but do not constitute direct measurements.

More recently, a modified ASL-MRI method was introduced⁴⁷ for non-invasive measurements of CSF production in mice. This promising technique directly shows the transport of water across the BCSFB in the CP. There is, however, still a need for the development of non-invasive methods which can be used to measure CSF production in humans.

1.2.3 Brain Waste Clearance in Health and Disease

In healthy individuals, CSF flow and waste clearance functions correlate strongly with sleep⁴⁸⁻⁵⁴, and have been observed to increase in the presence of low-frequency cerebrovascular oscillations (also referred to as vasomotion) associated with sleep, even in a state of wakefulness.^{55,56} Vasomotion has therefore been proposed as a major driving force of brain clearance. Other potential driving forces include cardiac pulsations and respiration, which induce pulsatile motion in vessels and tissue that have been linked to CSF flow patterns.^{57,58}

Impaired or disrupted waste clearance and CSF flow in the brain are associated with many neurological diseases. Hydrocephalus occurs when there is an excess of CSF which causes increased pressure in the cranium.^{34,59} The accumulation of waste products such as amyloid- β caused or aggravated by improper waste clearance can lead to Alzheimer's disease and cerebral amyloid angiopathy^{42,50,59,60}. Impaired waste clearance function is also associated with aging and neurodegenerative disorders in general^{42,52,61}. Therefore, the study of CSF production and flow in the human brain could lead to greater understanding of normal brain physiology and the conditions leading to disease, better monitoring of disease progression, and aid in clinical treatment decisions.

1.3 BRAIN PERFUSION

1.3.1 Definition and Importance

The human brain represents about 2% of total body weight but consumes up to 20% of its energy. In spite of this, the brain does not possess energy reserves itself, and therefore must be provided with a continuous supply of nutrients and oxygen through the blood. Halting the flow of blood to the brain for only a few minutes can lead to permanent damage to the tissue.⁶² The distribution of blood to the capillary bed of the tissue through the vasculature is referred to as blood perfusion, and it is measured in units of volume of blood per mass of tissue per time. In the brain, this is called cerebral blood flow (CBF) and its units are generally expressed in ml/100g/min. Since perfusion is such an important function for the brain, its study can reveal information about a number of pathologies such as stroke, arteriovenous malformations, brain tumours, neurodegenerative disorders, etc.⁶³⁻⁶⁵

1.3.2 Measuring Brain Perfusion

There exists an array of techniques which can measure brain perfusion. Rapid techniques allow time-resolved monitoring of perfusion changes, for example as a consequence of autoregulation behaviours or as a response to stimuli such as drug intake. Spatial resolution is necessary to show differences in perfusion between regions of the brain, which can detect pathologies that affect specific parts of the brain, such as hypoperfusion in stroke^{66,67}, or hyperperfusion and perfusion heterogeneities in tumours^{68,69}. CBF is higher in the gray matter (GM), where it averages 60 ml/100g/min in healthy individuals and lower in the white matter (WM), where it is approximately 20 ml/100g/min.⁷⁰ CBF differs with sex (females have a higher CBF on average) and aging decreases perfusion.⁷⁰⁻⁷² Popular methods for brain perfusion measurements include DCE-MRI, dynamic susceptibility contrast MRI (DSC-MRI), dynamic perfusion computed tomography (DPCT), and positron emission tomography (PET).⁷³⁻⁷⁵ DCE and DSC MRI employ intravenous Gd-based contrast agents which, as described in section 1.1.2, modify the magnetic properties of blood and the surrounding tissue. Changes in signal after injection can be visualized qualitatively, or converted to contrast agent concentration that can be the input to tracer kinetic models to extract quantitative parameters.^{76,77} A detailed description of DPCT and PET are beyond the scope of this work, however of note is that both techniques necessitate the use of ionizing radiation as well as injection of exogenous tracers, which is associated with heightened health risks.

In recent years, there has been a shift in paradigm in perfusion imaging towards newer techniques. This has been driven in part by concerns over the invasiveness of techniques requiring injection of contrast agents, the exposure to ionizing radiation in CT and PET, and the recent discovery of long-term deposition of Gd in tissue, particularly brain tissue, and the risk of development of nephrogenic systemic fibrosis after repeated examinations with MRI contrast agents.¹⁷⁻²⁰ Technical development in the field of ASL MRI, which does not have these disadvantages, and the publication of a white paper in 2015⁷⁸ creating a framework for standardized use, have increased its popularity and led to its wider acceptance and utilization in the clinic.⁷⁹⁻⁸⁴

1.4 ARTERIAL SPIN LABELING MRI

1.4.1 Introduction to Arterial Spin Labeling MRI

ASL is an MRI perfusion measurement technique which uses arterial blood water as an endogenous contrast agent. This makes it a completely non-invasive technique, with no need for contrast agent injection, and no exposure to ionizing radiation. Additionally, using water itself as the source of contrast ensures that measurements are done without external agents which may disturb the system we aim to characterize. It consists of a more direct measure-

ment of perfusion than MRI contrast agent methods which measure the indirect effects of these agents on the magnetization of water. Quantification of contrast agent concentration is also known to be quite difficult and DSC and DCE MRI are better suited to measure cerebral blood volume (CBV) than CBF.⁸⁵

The general principle behind ASL is to magnetically label (typically: invert the magnetization) the blood water as it enters the brain through the feeding arteries in the neck, and wait a certain amount of time to allow the labeled blood (or simply: label) to reach the capillary bed before imaging the brain. This is called a “label” image, which is subtracted from a “control” image where all imaging parameters are matched, but the inflowing blood is not labeled. In principle, the static tissue signal is the same in the control and label images, and the resulting subtracted ASL image contains only signal from blood water which has been labeled.⁷⁸ In reality, however, this subtraction is not perfect, and background suppression (BGS) pulses are applied to minimize the static tissue signal, thereby reducing physiological noise within the ASL-scan. The positive blood signal in the control image is effectively summed with the negative blood signal in the label image:

$$ASL\ signal = control\ signal - label\ signal = (Static\ tissue + blood) - (static\ tissue - blood) = 2 * blood\ signal \quad (Eq.\ 1.1)$$

ASL is usually acquired at relatively low spatial resolution (3 mm × 3 mm in-plane × 6 mm through-plane) to improve the signal-to-noise ratio (SNR), but even then the ASL image is typically noisy as the perfusion signal resulting from this technique represents only 1-2% of the total brain signal. To remedy this, the acquisition is repeated several times (~30 for a typical recommended implementation of ASL) and averaged to increase SNR.

A variety of methods fall under the umbrella of ASL, differing in the manner by which they label the blood, the background suppression approach, as well as the readout. These can be separated into three main categories. First, pulsed ASL (PASL) uses a single radiofrequency (RF) pulse with coverage over a large slab, positioned over the brain feeding arteries of the neck and up to the imaging region. This creates a spatial bolus of labeled blood, which is imaged 1.5-2.5 seconds after the labeling pulse, in order to allow time for the blood to reach the capillary bed.⁸⁶ A large number of diverse PASL techniques exist, with differences in the location of the labeling slab and the imaging region and other sequence characteristics to ensure matching of the magnetization transfer (MT) effects between the label and control conditions. Additional RF pulses may also be applied to create a more defined bolus length for quantification.⁸⁷⁻⁸⁹ Second, velocity selective ASL (VSASL) uses a combination of non-spatially selective RF pulses which label blood water based on the velocity (and sometimes acceleration) of the spins throughout the brain.⁹⁰⁻⁹³ By judiciously combining these pulses with varying encoding velocities and/or timing, specific regions of the vascular tree, such

as the capillary bed or venous blood vessels, can be isolated.⁹⁴ Since VSASL labels the blood directly in the spatial location where it is imaged, the transit time of the blood to the capillary bed is very short, and the waiting time between labeling and imaging that is used in other techniques can be drastically reduced, which improves SNR. VSASL can suffer from quantification issues because of the ill-defined bolus length, however additional velocity encoding modules may be applied to counter this, similar to what is used in PASL. The third category of ASL techniques, pseudo-continuous ASL (pCASL) is the one used in this work and will therefore be discussed in more detail in the next section (1.4.2).

Several techniques have been proposed for CBF quantification from the ASL signal⁹⁵⁻⁹⁸, but the implementation recommended in the ASL white paper⁷⁸ is the most commonly used, and it relies on a simplified equation which depends on only imaging parameters and subject specific parameters (typically using population averages).

1.4.2 Pseudo-Continuous ASL

In pCASL, a train of short, spatially selective RF pulses is applied in a thin slice (the labeling plane) intersecting with the brain-feeding arteries of the neck. The combination of RF pulses and magnetic field gradients at this slice allows for a process called flow-induced pseudo-adiabatic inversion to occur.⁹⁹ All spins which cross the labeling plane with a velocity within a pre-specified range are inverted, i.e. the magnetization of the inflowing blood is labeled. Figure 1.3 shows the positioning of the labeling plane and imaging region in a typical subject.

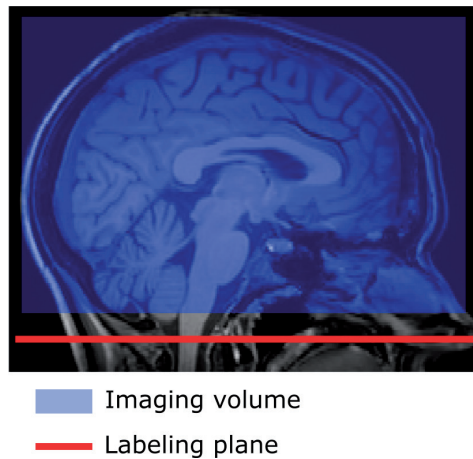


Figure 1.3. Schematic representation of the position of the labeling plane and imaging volume used in pCASL.

Prior to pCASL, continuous ASL (CASL) had been proposed.^{100,101} In this case, the RF was applied continuously during labeling, to result in a similar inversion. This however had significant disadvantages, as very few RF chains were designed to handle continuous usage and concerns arose as to power deposition in the subjects. Additionally, the considerable amount of RF power required induced large MT effects in the signal.¹⁰² These concerns were addressed by using a separate RF coil for labeling,^{103,104} however the need for additional hardware is in itself a limitation of the technique. Alternatively, amplitude-modulation could balance the MT effects between label and control condition, but this approach results in a lower labeling efficiency of approximately 60-70%, compared to a labeling efficiency around 85-90% for pCASL.¹⁰⁵ pCASL has since largely replaced CASL in the vast majority of applications as it can be performed on all MRI systems without requiring excessive power or additional hardware.^{106,107} pCASL has become the recommended labeling method for ASL since the publication of the white paper⁷⁸, because of its ease of implementation and improved SNR in comparison to PASL.

Instead of spatially labeling the bolus of blood, pCASL creates a bolus in time. The length of the bolus is determined by the amount of time that the inversion pulse train is applied, the labeling duration (LD). After the end of labeling, a short wait time of 1.5-2.5 seconds is inserted before reading out the imaging volume, to allow all labeled blood to travel up to the brain and reach the capillary bed. This time is called the post-labeling delay (PLD). Quantification of CBF in pCASL is done using this equation⁷⁸ :

$$CBF = \frac{6000 \cdot \lambda \cdot (S_{control} - S_{label}) \cdot e^{PLD/T_{1b}}}{2 \cdot \alpha \cdot T_{1b} \cdot S_{PD} \cdot (1 - e^{-LD/T_{1b}})} \quad (\text{Eq. 1.2})$$

Where $S_{control}$ and S_{label} are the signal in the control and label images, respectively, λ is the blood-brain partition coefficient¹⁰⁸, T_{1b} is the T_1 relaxation time of arterial blood, and α is the labeling efficiency of the pCASL labeling module. S_{PD} , also called M_0 , is the signal in the GM measured in a separate, proton-density weighted image and represents the equilibrium magnetization of GM. Single-voxel M_0 values or whole-brain averages may be used for quantification. This equation results in CBF values in units of ml/100g/min.

1.4.3 Choosing a PLD

A number of factors must be weighed when determining the optimal PLD to use with pCASL. During the PLD, two competing effects modify the signal intensity: the T_1 relaxation time of blood (T_{1b}), and the inflow time of labeled spins. After inversion of the blood water spins at the labeling plane, their longitudinal magnetization recovers, leading to the progressive loss of ASL signal. According to the Bloch equations¹⁰⁹ approximately 63% of the ASL signal is lost after a time equal to T_{1b} . T_{1b} is a constant, with small variations between subjects, and averages around 1650 ms.¹¹⁰ The time required for the blood to travel from the labeling

plane to the capillaries of the imaging voxel is referred to as the arterial transit time (ATT).¹¹¹ Typical ATTs for healthy brain tissue are around 1 s, with longer values in the border zones between brain regions, and white matter exhibits longer ATTs than gray matter.^{111–113} ATTs are longer in older populations, and in a number of pathologies including arteriovenous malformations, arterial stenosis and occlusion, Moyamoya disease, Alzheimer’s disease, and stroke.^{79,80,82–84,114–116} When acquiring perfusion-weighted images, the PLD should be set at a value that is long enough for the whole bolus of labeled blood to reach the capillary bed (i.e. longer than the longest ATT in the brain), in order to avoid signal in the arteries which creates high-signal artefacts and leads to CBF underestimation.

Therefore, the choice of PLD is a compromise: it must be long enough for all of the labeled blood to reach the capillary bed, and short enough to minimize signal loss through T_1 relaxation. The current recommendations for LD and PLD when using pCASL in healthy populations is LD = 1800 ms and PLD = 1800 ms.⁷⁸ These considerations hold for the measurement of perfusion images with a single PLD, however, other types of contrast may be desired. With shorter PLDs, the labeled blood still located in the arteries can be leveraged to acquire angiographic images, as was in fact one of the earliest applications of ASL.^{117–120} More recent studies have improved upon the technique and added features such as 4D-angiography and vessel-selective angiography.^{121–124} Multi-PLD protocols may also be useful. They can allow simultaneous quantification of CBF and ATT through dynamic modeling of the signal including the inflow phase of blood,^{125,126} or combined angiographic and perfusion imaging.^{127,128} A large number of short-PLD images can also create dynamic angiography images (aforementioned 4D-angiography).

1.4.4 Strategies for Acquisition at Multiple PLDs

Multiple “time points” (or combinations of LD and PLD) can prove useful to extract additional information from the ASL signal, other than CBF only. As previously mentioned, a multi-PLD protocol enables the measurement of the ATT. In the context of this work, multiple PLDs are also necessary to measure water exchange times from blood to other compartments in the brain such as GM and CSF.^{129–132}

The simplest and most obvious method to acquire multiple PLDs is with separate sequential scans within the same scan session, each with a different PLD (and/or LD). This is generally an inefficient use of time, with each scan lasting several minutes to provide a single time point. Figure 1.4 shows ASL signal at multiple time points acquired sequentially. We can observe the change in contrast with increasing LD and PLD. In early time points the signal is in the large arteries, then it travels to the tissue to result in a perfusion image before decaying at longer time points.

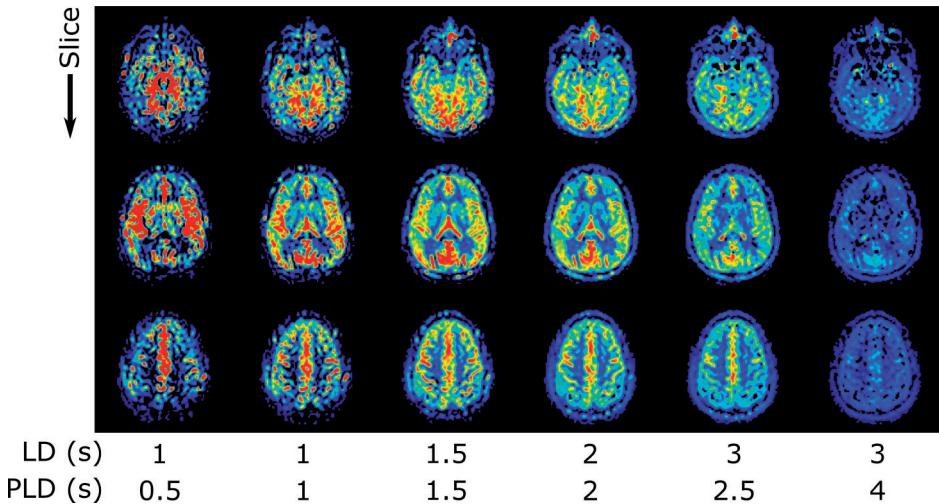


Figure 1.4. Example dataset with sequential acquisition of 6 time points with LD and PLD values indicated at the bottom. The three rows show three different slices of the brain.

A faster method is the Look-Locker readout which applies a series of low-flip-angle excitation pulses in between fast EPI acquisitions, allowing the measurement of ASL signal at multiple PLDs following one labeling module. Flip angles and timings between pulses can be optimized for better quantification of perfusion parameters. This method requires modifications to the pre-existing perfusion models to take into account the perturbations induced in the ASL signal by the train of excitation pulses.^{113,133–137} ASL fingerprinting has also been proposed for the fast simultaneous measurement of multiple perfusion parameters.¹³⁸

Time-encoded or Hadamard-encoded ASL uses judicious ordering and timing of the label and control images to acquire multiple time-points in a time-efficient manner.^{139–141} The time allotted for labeling is separated into blocks of a given length followed by a single short PLD, and these blocks alternate between the label and control condition according to a Hadamard matrix scheme. Hadamard matrices are square and of order N , where N is 1, 2, or a multiple of 4, and each element of the matrix is either 1 or -1, associated with the label or control condition respectively. In ASL, Hadamard matrices of order 4, 8, or 12 are most frequently used (see figure 1.5 A for an example of acquisition with Hadamard-encoding of order 4). For a Hadamard matrix of order N , each image is acquired with $N-1$ blocks of label or control (the first column of the matrix where the label condition is the same for all blocks is discarded). The acquisition is repeated N times, and the label and control conditions are varied to complete the matrix. Block lengths can vary, but repeated acquisitions of the same blocks must have the same length, i.e., in figure 1.5 A, blocks 1, 2, and 3 may have different lengths, but all blocks labeled 1 (or 2 or 3) have the same length. To retrieve the ASL signal, the N images are added and subtracted in a decoding step according to the

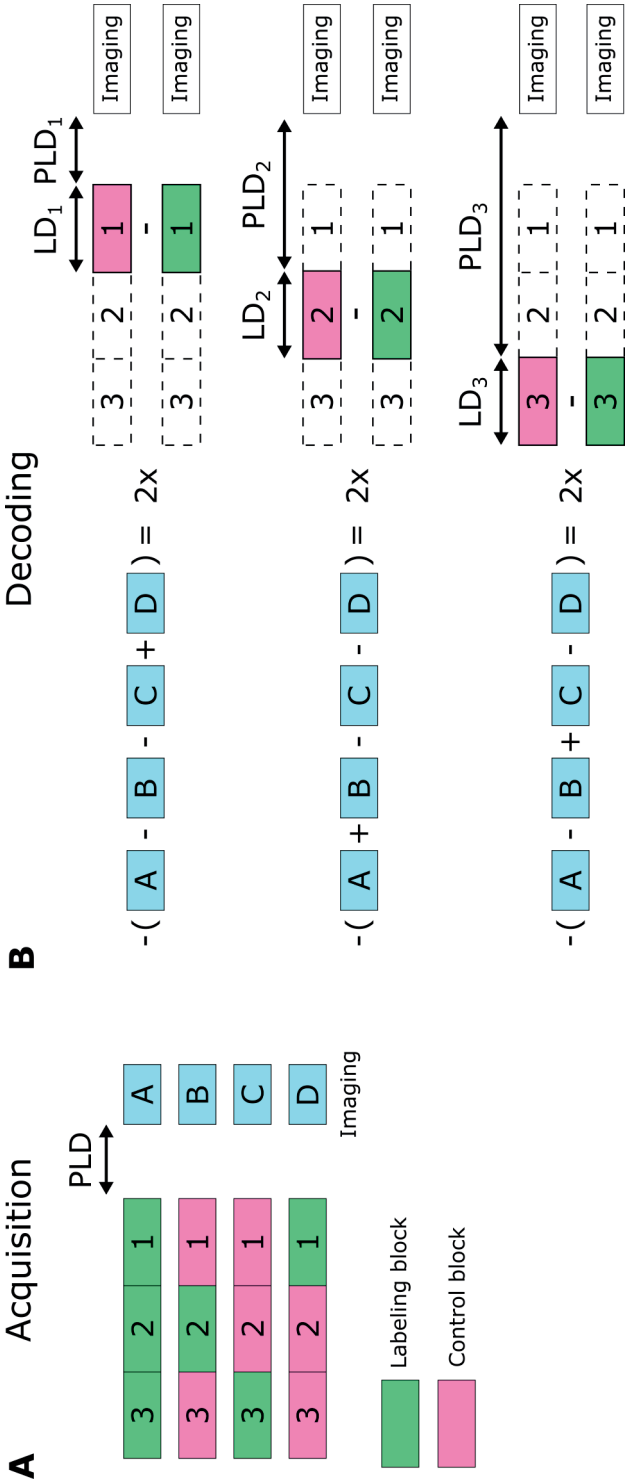


Figure 1.5. Time-encoded ASL acquisition scheme with Hadamard-4 matrix (A) and the 3 time points resulting from decoding with their associated LDs and PLDs (B).

Hadamard matrix scheme (figure 1.5 B). The result is equivalent to the acquisition of N-1 ASL images with LD = block duration and effective PLD = sum of duration of subsequent blocks + minimum PLD. This is shown in figure 1.5 B for a Hadamard matrix of order 4 resulting in 3 time points. To measure each of these N-1 time points sequentially, $2 \times (N-1)$ acquisitions are necessary (1 label image and 1 control image for each time point), while with Hadamard only N acquisitions are needed. This significantly reduces scan time, especially for the acquisition of short LD/PLD time points, without reducing SNR.

Block timings can be adjusted depending on the desired type of contrast or optimized for the measurement of a given parameter. One example of an acquisition scheme is the so-called “free lunch” approach,¹⁴¹ where the first block of the Hadamard matrix (number 3 in figure 1.5) is the full length of the LD of a normal single-PLD perfusion image (e.g. 1800 ms), and what would usually be just a wait time without labeling during the PLD (1800–2000 ms) is in this case separated into shorter blocks. As a result, a perfusion image with the same SNR as when acquiring a normal single-PLD perfusion scan of the same total scantime is obtained, but with as additional output several shorter PLD images that sample the inflow of blood and allow for quantification of both CBF and ATT.

1.4.5 Acquisition at Multiple Echo Times

Multiple echo times (TE) can be acquired in MRI to sample the T_2 relaxation curve of the signal. In general, the purpose of this is to map the T_2 values in the imaging volume. Within the scope of ASL, multi-TE protocols are used to separate the total signal into its components originating from different compartments based on the difference in T_2 values of these compartments.^{142,143} Traditionally, the relevant compartments in ASL are blood and gray matter, and in this work we introduce ASL measurements in a third compartment, the CSF. Blood T_2 varies from 100–250 ms depending on hematocrit and oxygenation^{144–146}, GM T_2 is 70–100 ms^{145,147,148}, and CSF has an exceptionally long T_2 at around 1500 ms.¹⁴⁹

Figure 1.6 shows the T_2 decay of signal in blood, GM, and CSF. At shorter TEs (50 and 100 ms are shown), the contrast between blood and GM is greatest, at longer TEs (800 ms), blood and GM signals are virtually suppressed, allowing the isolation of the CSF signal.

Acquiring multiple TEs is done in one of two ways: using a multi-echo readout, or a $T_{2\text{prep}}$ module. Multi-echo acquisition is faster, as it measures the signal at multiple echo times sequentially in a single acquisition of the volume, however, it necessitates a large inter-echo spacing. For a shorter inter-echo spacing, only a small portion of the matrix can be measured during each readout, leading to a larger number of readouts necessary to complete the acquisition of a single image, resulting in lengthy acquisition and increasing the risk of motion artifacts. More explanations on the topic of multi-echo readout are found in **chapter 3**.

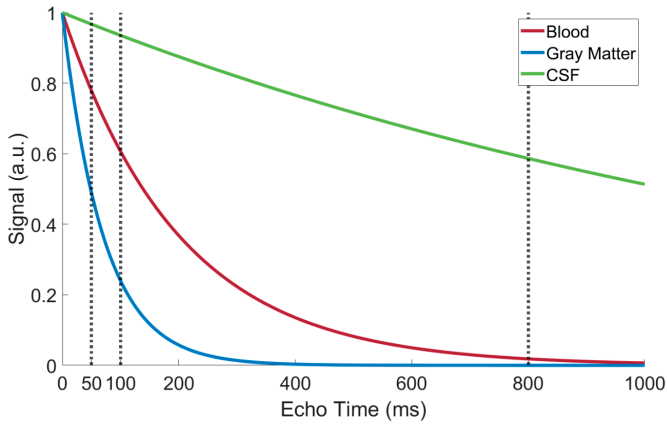


Figure 1.6. T_2 relaxation curves for blood (200 ms), GM (70 ms) and CSF (1500 ms) at 3T

When shorter echo times are necessary, such as when separating blood and GM signals, a $T_{2\text{prep}}$ module is frequently used. This consists of a train of RF pulses inserted before the excitation which induces T_2 decay for a set length of time before flipping the magnetization back into the longitudinal direction. The T_2 -module thereby increases the effective echo time of the sequence. For this technique, the acquisition of the entire image is repeated with different $T_{2\text{prep}}$ modules (i.e. different effective echo time), thus making it more time-consuming than multi-TE. More information about $T_{2\text{prep}}$ and its applications in ASL is found in **chapter 2**.

1.5 INTRODUCTION TO THIS WORK

This thesis focuses on the measurement of water exchange across the BBB and BCSFB with ASL. All the theoretical building blocks of the employed techniques have been introduced in this chapter. **Chapter 2** presents a direct comparison of existing ASL techniques for the assessment of BBB integrity. **Chapter 3** introduces a new method for the measurement of BCSFB water exchange in humans using ASL. **Chapter 4** examines the ramifications of the presence of ASL signal in the CSF for estimates of CBF using partial volume correction. **Chapter 5** aims to combine the BBB and BCSFB measurement methods into one scan for a comprehensive view of water exchange in the brain. In **Chapter 6** we present a general discussion of all the results in this work and their implications for our understanding of brain function and clearance.